quirements: 1) it must operate in a single-mode or controllable-multimode fashion to prevent signal distortion, 2) it must have large dimensions to facilitate excitation and 3) it must have practical tolerances and size to permit component fabrication. The successful operation of a waveguide medium meeting these requirements has recently been demonstrated at Wheeler Laboratories.

The technique employed utilizes dielectric waveguides formed by imbedding, in a transparent medium, a dielectric core of slightly higher dielectric constant. These waveguides, which are well known at microwave frequencies,[1] can support a finite number of propagating modes and an infinite number of leaky (or radiating) modes. The propagating modes comprise plane waves which are incident on the dielectric interface at angles between the critical angle of the dielectric interface and grazing incidence; therefore, these waves experience total internal reflection and propagate along the waveguide with small losses. The leaky modes comprise plane waves which are incident between the critical angle and normal incidence; at each reflection there will be a refracted wave in addition to a reflected wave so that the energy propagating down the waveguide is highly attenuated. The condition for lossless propagation depends on the dimensions of the core dielectric medium and on the difference in dielectric constants across the interface. For the case of slab-waveguide geometry, the thickness of the slab required for propagation of the mode of order m is

$$d \geq D_m = \frac{m}{\sqrt{k_1 - k_2}} \frac{\lambda}{2}. \qquad (1)$$

Here d is the thickness of core dielectric, D_m is the critical thickness for the propagating mode of order m; k_1, k_2 are the dielectric constants of the core and outer media, respectively, and λ is the optical wavelength. The lowest mode has m equal to zero and will propagate in slabs of arbitrary thickness.

Eq. (1) indicates one technique for providing a single-mode optical waveguide with macroscopic dimensions. If $k_1 - k_2$ is small, D_1 will be many wavelengths. By choosing d slightly less than D_1 only the dominant mode ($m=0$) will propagate; all higher modes will be attenuated. The term macroscopic has been applied to such a waveguide to indicate that the dimensions are at least one order of magnitude greater than the optical wavelength, so that the waveguide would be visible with the naked eye.

A typical waveguide of this type may be described as follows: The outer dielectric comprises two optically flat, precision-annealed glass plates. These are mounted parallel within 0.1 milliradian; the spacing between them is of the order of 10 to 100 microns and can be controlled to 1.0 micron. The core medium is obtained by filling the space between the plates with a transparent liquid mixture having a dielectric constant slightly higher than that of the glass. A liquid core is employed to provide a smooth interface and to permit accurate control of the difference in dielectric constants across the interface. This is accomplished first by mixing two liquids with dielectric constants which bridge that of the glass, and second by accurate control of temperature.

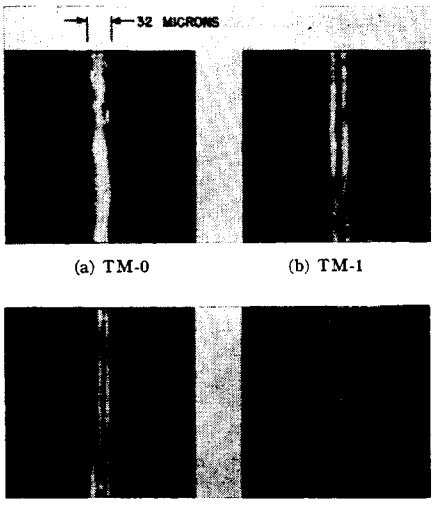

(a) TM-0 (b) TM-1

(c) TM-2 (d) TM-3

Fig. 1—Mode patterns in macroscopic optical waveguide (dielectric-slab configuration).

An experimental waveguide, fabricated at Wheeler Laboratories, utilizes glass plates with $k_2 = 2.2952$, spaced 32 microns (50 wavelengths of red light) apart. A mixture of benzene ($k=2.2440$) and chlorobenzene ($k=2.3104$) provides a core medium with dielectric constant slightly above that of the glass. The required difference in dielectric constants for single-mode operation is 0.00010; this is provided by small variations in temperature since the constant of the liquid changes by 0.001/°C. Temperature control to 0.1°C was provided during testing. The waveguides are 77 mm long.

This waveguide was excited with a helium-neon gas laser operating at 633 millimicrons. The beam was collimated and fed directly into one end of the waveguide at a controlled angle of incidence. The polarization was perpendicular to the plane of the slab so that TM modes are excited.

The observed modes of the waveguide are shown in Fig. 1. These photographs were taken through a microscope, focused on the end of the waveguide, and show the field patterns propagated in the guide. The dielectric constant of the liquid core was first adjusted to provide four modes of operation ($k_1 - k_2 = 0.0020$). For normal incidence of the laser beam the single TM-0 mode was observed as in Fig. 1(a). As the angle of incidence was increased in either direction the higher modes of this waveguide were successively observed as shown in Figs. 1(b) through (d). If the angle of incidence was increased beyond that angle for which the TM-3 mode is excited, the waveguide was dark. This is because all the higher modes which are excited are severely attenuated through the experimental length of waveguide. With the dielectric constant of the liquid core adjusted for single-mode operation ($k_1 - k_2 = 0.00010$), only one line could be observed as the incident angle of the laser beam was varied from normal incidence to about 10 milliradians. This is the TM-0 mode shown in Fig. 1(a). Above this angle the waveguide does not propagate, therefore, single-mode operation is obtained.

These experiments have clearly demonstrated the ability to control modes in an optical waveguide of large dimensions or to fabricate a single-mode macroscopic optical waveguide. Although this configuration was found useful for experimental work, other, more practical configurations for component design are being considered.

The author wishes to acknowledge the assistance of D. W. Wilmot in the evaluation of various configurations and R. W. Hermansen who performed the experiments described above.

ROBERT A. KAPLAN
Wheeler Laboratories, Inc.
Great Neck, N. Y.

[1] R. E. Collin, "Field Theory of Guided Waves," McGraw-Hill Book Company, Inc., New York, N. Y. 1960.

Power-Law Nature of Field-Effect Transistor Experimental Characteristics*

In making experimental measurements of field-effect transistor static drain characteristics in the pinch-off region, determination of the effective pinch-off voltage is not possible by direct measurement because of the presence of spurious drain current at and beyond pinch-off. Further, indirect measurement is hampered by the absence of a theoretical straight-line function from which the pinch-off voltage may be obtained as an intercept or a slope. In this communication a power-law relation for the transfer characteristic is assumed, from which values of both the pinch-off voltage and the exponent may be obtained directly from a straight-line plot of experimental quantities.

In an accompanying communication,[1] a square-law dependence of drain current I_d upon gate voltage V_g is derived by a simple theoretical argument. In view of the approximations inherent in this derivation, it is reasonable to suppose that an arbitrary power law would provide a somewhat better approximation to the actual transfer characteristics in the pinch-off region. Let this relation be expressed as

$$I_d = I_{d0}\left(1 + \frac{V_g}{V_p}\right)^n \qquad (1)$$

where I_{d0} is the drain current at zero-gate voltage, V_p is the pinch-off voltage and n is expected to be close to 2. For p-n junction (FET's) field-effect transistor, V_g is restricted to negative values. By differentiation, the small-signal transconductance g_m is given by

$$g_m \equiv \frac{dI_d}{dV_g} = \frac{nI_{d0}}{V_p}\left(1 + \frac{V_g}{V_p}\right)^{n-1} \qquad (2)$$

* Received May 13, 1963. The work reported here was supported in part by funds made available by the Jet Propulsion Laboratory, California Institute of Technology, Pasadena, under NASA Contract No. NAS 7-100.

[1] R. D. Middlebrook, "A simple derivation of field-effect transistor characteristics," this issue, pp. 1146–1147.

and so the ratio

$$\frac{I_d}{g_m} = \frac{1}{n}(V_p + V_g) \qquad (3)$$

should give a straight line when plotted on linear scales as a function of V_g. Further, the pinch-off voltage and the exponent are obtained directly as the intercept on the voltage axis and the reciprocal slope of the straight line.

Plots of (3) for p-n junction FET's of various structures are shown in Fig. 1, and the resulting values of V_p and n are given in Table I. It is seen that the experimental points do indeed define straight lines quite closely, thus vindicating the postulated power-law relation of (1). Moreover, the values of n obtained are reasonably close to 2, thus lending weight to the simple theoretical square-law derivation of the accompanying communication. The departure from a straight line in some units near the pinch-off voltage is due to drain leakage current, and is the effect that prevents direct measurement of the pinch-off voltage. The maximum in I_d/g_m that occurs at small positive gate voltages is to be expected on theoretical grounds, and is not significant in determining the best-fit straight line over the range $0 < |V_g| < V_p$.

It is concluded that the power-law relation of (1) satisfactorily represents both theoretically and experimentally the transfer characteristics of an FET in the pinch-off region, and allows values of the pinch-off voltage and the exponent to be determined directly from experimental measurements.

A future communication will show theoretically why the values for the exponent n obtained experimentally are so close to the value 2 derived by the approximate treatment in the accompanying communication.

The authors wish to thank Texas Instruments Inc., and Motorola Inc., who kindly supplied some of the units used for the measurments here reported.

I. Richer
R. D. Middlebrook
Div. Eng. and App. Sci.
California Institute of Technology
Pasadena, Calif.

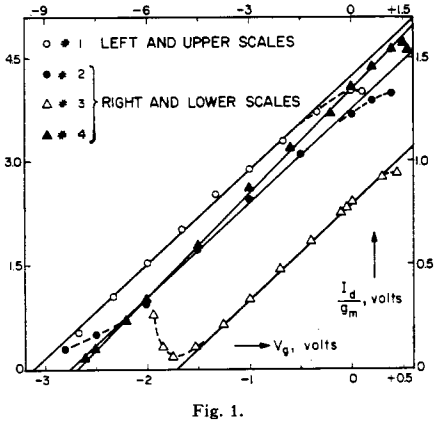

Fig. 1.

TABLE I

Measurement Conditions: Frequency = 1 kc
$|V_d| = 25$ v (#1), $|V_d| = 10$ v (#2–#4)

Unit	Type	Nature of junction	V_p volts	n
#1	Crystalonics 610	alloy (n-channel)	9.33	2.20
#2	Motorola MM 764	epitaxial (n-channel)	2.74	2.18
#3	Texas Instruments TIX 691	diffused (p-channel)	1.70	2.15
#4	Fairchild FSP 401	diffused (n-channel)	2.68	1.98

A Simple Derivation of Field-Effect Transistor Characteristics*

In the conventional treatment of the field-effect transistor, the first step is the specification of an impurity profile that describes the nature of the gate-channel contact. Solutions for the static and small-signal characteristics are then valid only for the particular impurity profile chosen, and must be repeated from the beginning for different structures.

The purpose of this communication is to present a simple, though approximate, development of the characteristics of an FET without specifying the detailed nature of the structure. The charge-control approach is used,[1,2] and it is shown that in the pinch-off region the relation between the drain current and the gate-source voltage is approximately square law. The results are applicable to all gate-channel structures, including the insulated gate types.

The basic model of an n channel FET (field-effect transistor) is shown in Fig. 1. One-dimensional current flow in the channel of length L is assumed to occur under the influence of a drain-source voltage V_d and a gate-source voltage V_g. The method of solution is to calculate the drain current I_d from the fundamental charge-control relation $I_d = Q/\tau_t$ where τ_t is the average transit time of the mobile carriers making up the total charge Q in transit between source and drain. The total mobile charge Q in the channel can be considered as made up of two parts: one part, Q_c, is the charge which would exist in the absence of the gate structure; the other part, Q_g, is the additional charge induced by a gate voltage.

The basic simplifying assumption to be made is that the potential drop in the channel is uniform so that the electric field is constant and equal to V_d/L. If the mobile carriers have constant mobility μ, the drift velocity is constant at $\mu V_d/L$ and the transit time is $\tau_t = L^2/\mu V_d$. The drain current is $I_d = (Q_c + Q_g)/\tau_t = G_c(1 + Q_g/Q_c)V_d$ where $G_c \equiv \mu Q_c/L^2$ is identified as the channel conductance in the absence of the gate structure, and in which the additional charge Q_g may be expressed as a function of the average voltage between gate and channel. Under the assumption of constant channel field, this average voltage is $(V_g - V_d/2)$ and the additional channel charge may be written $Q_g = C_g(V_g - V_d/2)$ where C_g represents a capacitance which, under certain conditions, may be identified as the total gate capacitance. Hence the drain current is given by

$$I_d = G_c\left(1 + \frac{V_g - V_d/2}{Q_c/C_g}\right)V_d. \qquad (1)$$

The above equation describes approximately the drain characteristics of the device in the region where the incremental drain conductance $\partial I_d/\partial V_d$ is finite, as indicated in Fig. 2. From the above equation, the drain conductance is

$$\frac{\partial I_d}{\partial V_d} = G_c\left(1 + \frac{V_g - V_d}{Q_c/C_g}\right) \qquad (2)$$

which goes to zero when $V_d - V_g = Q_c/C_g$. The drain current for which the drain conductance is zero is therefore given as a function of gate voltage by substitution of this condition on V_d back into (1), which leads to

$$I_d = \frac{G_c}{2}\frac{Q_c}{C_g}\left(1 + \frac{V_g}{Q_c/C_g}\right)^2 \qquad (3)$$

If the gate voltage is chosen so that $V_g = -Q_c/C_g$, the drain current is zero and

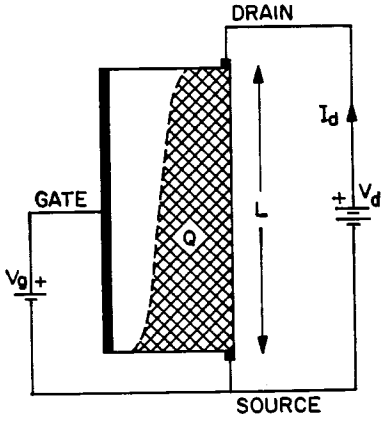

Fig. 1.

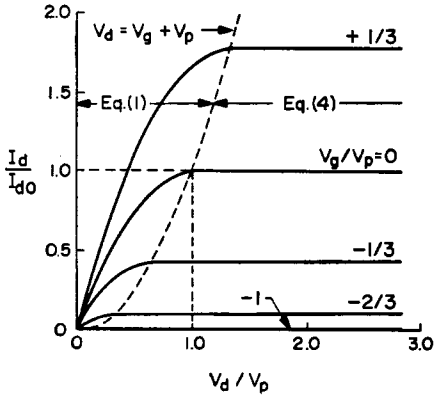

Fig. 2.

* Received May 13, 1963. The work reported here was supported in part by funds made available by the Jet Propulsion Laboratory, California Institute of Technology, Pasadena, under NASA Contract No. NAS 7-100.

[1] E. O. Johnson and A. Rose, "A simple general analysis of amplifier devices with emitter, control, and collector functions," Proc. IRE, vol. 47, pp. 407–418; March, 1959.

[2] R. D. Middlebrook, "A modern approach to semiconductor and vacuum device theory," *Proc. IEE*, vol. 106, pt. B, suppl. no. 17; pp. 887–902; May, 1959.